# THEORETICAL MODEL FOR COMPOSITE BEAMS WITH A FLEXIBLE BOND LAYER

**Laila M. El-Hifnawy, Mohamed A.F. Diwan**
**Structural Engineering Department, Faculty of Engineering, Alexandria University, Alexandria, Egypt.**

**and Nahed S.A. Zaghloul**
**The General Authority for Public Buildings, Alexandria Governorate.**

ABSTRACT

**This paper introduces a theoretical analysis of beams with composite sections. The considered composite section consists of two materials bonded together by a flexible bond layer. The top profile material has a flexural rigidity and the bottom one has an axial resistance only. Relative shear deformation of the bond material is considered. The differential equations of the proposed model are developed and then solved theoretically. Two methods of solution have been used. These are the transport matrix method and the finite element method. The solution methods are extended in order to solve frames as well as beams. Sandwich beams with top profiled face and reinforced concrete beams strengthened by epoxy-bonded steel plates are two types of examples which have been used to verificate the theoretical model. Comparisons between the theoretical model and the available experimental results show good agreement. Also, design curves of sandwich beams are given for different cases of loading and different boundary conditions.**

***Keywords: Composites, Structural Analysis.***

*Notations*

$E_1$ modulus of elasticity of top element
$E_2$ modulus of elasticity of bottom element
$I_1$ second moment of area of top element
$A_2$ cross-section area of bottom element
a distance between centres lines of top and bottom elements
g bond width
t thickness of bond material
p applied uniform load
w deflection of beam element
$\phi$ angle of rotation due to bending
$\gamma$ net angle of rotation
$\delta_B$ relative displacement due to bending
$\delta_N$ relative displacement due to acting normal force on both elements
$\delta$ total relative displacement between top and bottom elements of composite beam
G shear modulus of bond material
M bending moment of beam section
$M_1$ bending moment of top element
$M_2$ bending moment of bottom element
Q shear force of beam section
$Q_1$ shear force of top element
$Q_2$ shear force of bottom element
q shear force of bond material
N normal force
$p_e$ distributed peeling force (normal force of bond material)
V state vector matrix
T transport matrix
I unit matrix
P load vector matrix
$P_t$ point matrix
$\bar{k}$ local stiffness matrix
k global stiffness matrix
$T_r$ transformation matrix
$T_r^t$ transpose of the transformation matrix
$\bar{\Delta}$ local deformation matrix
$\Delta$ global deformation matrix
$\bar{F}$ local force matrix
F global force matrix

INTRODUCTION

Composite sections can combine the advantages of lightness, stiffness, strength and, also, excellent thermal properties. Examples are: a- sandwich panel or beam composed of metal faces of steel or aluminum and a rigid foam core, and b- aluminum alloy reinforced by adhesive bonding of carbon fiber/epoxy composites. These sections may have different uses in the aircraft industry and military or civil structures.

On the other hand, existing concrete structures may, for a variety of reasons, be found to be unsatisfactory under service loading. This could manifest itself by poor performance in the form of excessive deflections or cracking. One method which has considerable potential in the strengthening field is that which involves the bounding of steel plates to the surfaces of the members to be strengthened. Figure (1) shows typical cross-sections of the mentioned examples of composite Structures.

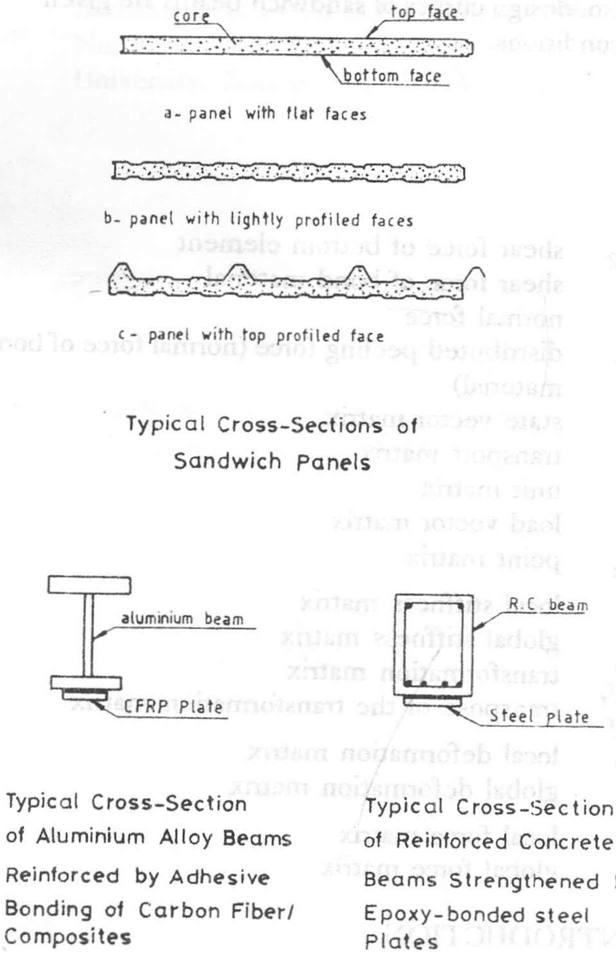


Figure 1.

The bending behavior of a general sandwich beam, delaminated (debonded) at one of the skin-core interfaces with transversely flexible core has been studied by many researchers such as Y. Frostig [1]. His analysis considered a two-dimensional formulation for the core, in longitudinal and transverse directions, combined with a beam theory formulation for the skins. The effects of the vertical flexibility of the core, in the undelaminated and the delaminated regions on the behavior are considered.

O. Vilnay [2], studied the behavior of aluminum alloy struts and beams reinforced by CFRP. He investigated the failure due to cracking of the adhesive bond, in addition to the shear and the peeling stress in the aluminum beams reinforced by CFRP .

T.V. Parry and R.S. Wrenski [3] carried out several tests on aluminum alloy beams selectively reinforced on one or both surfaces with uniaxially aligned continuous CFRP.

F.J.H. Tutt, Bsc. and Mimeehe., [4] examined aluminum flanges of the deck unit of military bridges. They designed and manufactured four light alloy beam specimens in order to test the behavior of the adhesive and the selective reinforcement.

For the strengthening of concrete structures by bonding steel plates to concrete surfaces, R.Jones, R.N. Swamy, and A. Charif., [5] studied the problem of using anchors at the ends of steel plates which is glued to the tensile faces of reinforced concrete beams. They presented a simple theoretical study of the force systems at the plate, glue and the glued concrete interfaces. They discussed the efficiency of the different anchorage details, and they showed that the use of additional glued anchor plates gives the best results. These plates overcome the problem of anchorage failure and enable the full theoretical flexural strength to be achieved, together with ductile behavior.

T.M. Roberts.m [6] presented a simple approximate procedure for predicting the shear and normal stress concentrations in the adhesive layer of reinforced concrete beams strengthened by glued steel plates.

This work presents the theoretical analysis of the composite beams. The composite sections consist of two materials bonded together by a flexible bond layer. The top profile element has a flexural rigidity and the bottom profile element has an axial resistance only. The theoretical model and the governing differential equations are presented.

Two methods of solution have been approached considering the relative shear deformation of the bond material. These methods are the transport matrix method and the finite element method.

Verification of the theoretical model is performed Solutions of sandwich beams with top profiled face and reinforced concrete beams strengthened by epoxy-bonded steel plates are presented and compared with the available experimental results. The comparisons show a good agreement between the theoretical predictions and the experimental results.

Design curves of sandwich beams are given for different cases of loading and different boundary conditions.

## EQUILIBRIUM EQUATIONS:

Figure (2) shows a differential element of a composite beam segment of length dx with the internal force acting on it together with the external distributed load p. The following major assumptions are considered:

1- The materials of the elements are elastic-homogeneous and isotropic.
2- The strain in the top element is due to bending while the strain in the bottom element is due to axial force only.
3- Peeling force (normal force) of the bond element is negligible.
4- The shear resistance to external loads is provided by the top element only.
5- First order theory is considered.

The total shearing force Q and bending moment M are equal to:

$$Q = Q_1 \tag{1}$$

$$M = M_1 + N.a \tag{2}$$

in which (a) is the distance between the center lines of the top and the bottom elements. Due to the beam theory, the relation between the total moment and the external distributed load is given by

$$\frac{d^2M}{dx^2} = -p \tag{3}$$

The relation between the moment and the curvature can be expressed as:

$$M_1 = - E_1 I_1 \frac{d\phi}{dx} \tag{4}$$

in which $E_1$ is the modulus of elasticity of the top element, $I_1$ is the second moment of area of the top element and $\phi$ is the angle of rotation of the composite beam due to bending which is given by:

$$\phi = \frac{dw}{dx} \tag{5}$$

where w is the deflection.

Relative shear deformations between the top and bottom elements are shown in Figure (3) where the total relative displacement $\delta$ can be expressed as:

$$\delta = \delta_B + \delta_N \tag{6}$$

where $\delta_B$ is the relative displacement due to bending and $\delta_N$ is the relative displacement due to the acting normal force on both elements.

From Figure (3):

$$\delta_B = a.\,\phi \tag{7}$$

and

$$\gamma = \phi - \frac{\delta}{a} \tag{8}$$

where $\gamma$ is the net angle of rotation of the composite section.

Two times differentiation of equations (6) and (7) gives:

$$\frac{d^2\delta}{dx^2} = \frac{d^2\delta_B}{dx^2} + \frac{d^2\delta_N}{dx^2} \tag{9}$$

$$\frac{d^2\delta_B}{dx^2} = a.\frac{d^2\phi}{dx^2} \tag{10}$$

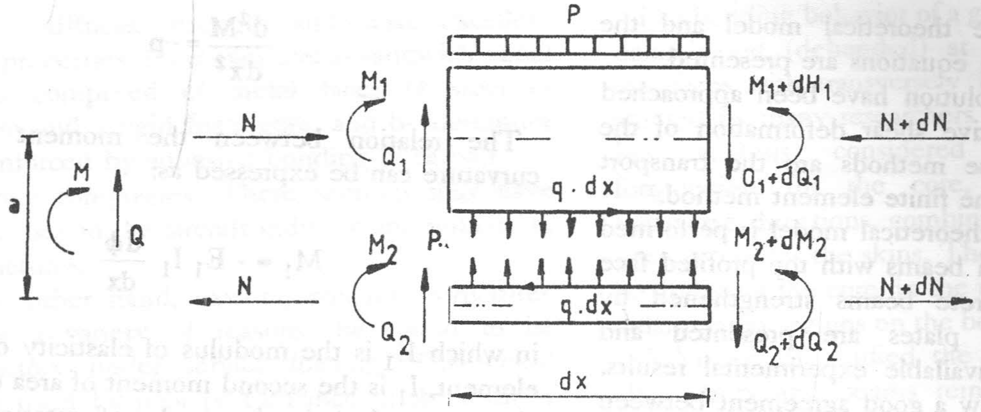


Figure 2. Differential element of the composite beam.

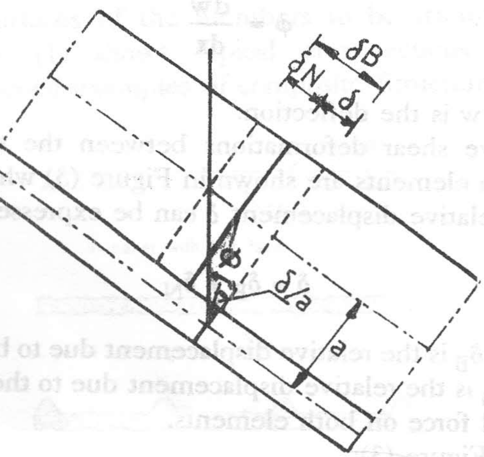

Figure 3. Relative displacement between top and bottom elements.

The strain due to the axial force can be expressed as:

$$\epsilon = \frac{d\delta_n}{dx} = \frac{N}{E_2 A_2} \quad (11)$$

in which $E_2$. $A_2$ are the modulus of elasticity and the cross-section area of the bottom element, respectively.
Differentiation of equation (11) yields:

$$\frac{d^2\delta_N}{dx^2} = \frac{1}{E_2 A_2} \cdot \frac{dN}{dx} \quad (12)$$

Substituting equations (10) and (12) into equation (9) results in:

$$\frac{dN}{dx} = E_2 A_2 \left[ \frac{d^2\delta}{dx^2} - a \frac{d^2\phi}{dx^2} \right] \quad (13)$$

Considering the equilibrium of the top or the bottom element in the horizontal direction, then the shear force of the bond element is:

$$q = \frac{dN}{dx} = G' . \delta \quad (14)$$

in which $G' = \frac{G.g}{t}$ where G is the shear modulus of the bond material, g and t are the bond element width and thickness, respectively.
Substituting equations (5) and (14) into equation (13), then

$$\delta'' - \omega^2 \delta = a\, w''' \quad (15)$$

where

$$\omega^2 = \frac{G'}{E_2 A_2}$$

Differentiating equation (2) twice, and equations (9) and (10) once, and substituting in each other yields:

$$\frac{d^3\delta_N}{dx^3} = \frac{d^3\delta}{dx^3} - a \frac{d^4 w}{dx^4} \quad (16)$$

Substituting equations (3), (4) and (16) using the differentiation of equation (12) into the second differentiation of (2) then

$$w^{IV} - \frac{\alpha_1^2}{a}\delta''' = \frac{p}{\alpha_2} \quad (17)$$

where

$$\alpha_1^2 = \frac{a^2 E_2 A_2}{E_1 I_1 + a^2 E_2 A_2}$$

and

$$\alpha_2 = E_1 I_1 + a^2 E_2 A_2$$

Equations (15) and (17) are coupled differential equations.

By differentiations and substituting result the two uncoupled differential ones, equations (18) and (19)

$$\delta''' - \Omega^2 \delta' = \alpha_3 \quad (18)$$

where

$$\Omega^2 = \frac{\omega^2}{1-\alpha_1^2} \text{ and } \alpha_3 = \frac{p.a}{\alpha_2(1-\alpha_1^2)}$$

$$w^{VI} - \Omega^2 w^{IV} = \alpha_4 \quad (19)$$

where

$$\alpha_4 = \frac{-p\Omega^2}{\alpha_2}$$

The solution of equations (18 and 19) gives

$$w_x = A_1 \sin h\, \Omega x + A_2 \cosh \Omega x + A_3 x^3 + A_4 x^2 + A_5 x + A_6 + \frac{p}{24\alpha_2} x^4 \quad (20)$$

$$\delta_x = A_1 \frac{a\Omega}{\alpha_1^2}\cosh \Omega x + A_2 \frac{a\Omega}{\alpha_1^2}\sinh \Omega x - A_3 \frac{6a}{\omega^2} - \frac{p.a}{\alpha_2 \omega^2} x \quad (21)$$

where $A_1$ to $A_6$ are coefficients which depend on the boundary conditions.

Other deformations and forces equations of the beam can be obtained according to their definitions.

## METHODS OF ANALYSIS

### *Transport Matrix Method*

In the transport matrix method, the beam is divided into a number of elements which are connected together at discrete joints. Then, the transport matrices are formulated for these elements. Besides, the solution is extended to handle portal frames by introducing point matrices at frame corners. Also in case of concentrated deformations or forces at any joint, a corresponding point matrix is used to overcome this problem.

The deformations and forces at any section at distance x from the starting point, x =0, can be obtained as a function of the deformations and forces at that point.

Solving equations (20,21) for x=0 and by rearranging, the developed equations are written in a matrix form as:

$$\{V_x\} = [T]\{V_o\} \quad (22)$$

$V_o$: State vector represents the deformations and forces at x =0

$$= < w_o\ \gamma_o\ \delta_o\ M_o\ (M_1)_o\ Q_o\ 1.0 >_{7x1}$$

$V_x$: State vector represents the deformations and forces at any section at distance x from the starting point.

$$= < w_x\ \gamma_x\ \delta_x\ M_x\ (M_1)_x\ Q_x\ 1.0 >_{7x1}$$

T: Transport matrix which relates the vector $V_x$ to the vector $V_o$.

it is given in Appendix A.

### *Finite Element Method*

The second method of solution is the finite element method which has become a powerful tool of analyzing a wide range of problems. In the present analysis, the element stiffness matrix, $\bar{k}$, is the derived directly from the transport matrix obtained in the previous sub section. Then the global stiffness matrix and its solution are generated following the standard steps of the finite element method.

Equations (22) giving the deformations and forces (except the axial ones) for a beam element of length x, Figure (4) can be rearranged to take the form:

$$A.\bar{F} = B.\bar{\Delta} \quad (23)$$

where

$\bar{F}$ = local end forces of the element at nodes 1 and 2

$= < \bar{F}_1 \bar{F}_2 >$

$= < Q_1 M_1 (M_1)_1 Q_2 M_2 (M_1)_2 >_{6x1}$

$\bar{\Delta}$ = local end deformations of the element at nodes 1 and 2

$= < \bar{\Delta}_1 \bar{\Delta}_2 >$

$= < w_1 \gamma_1 \delta_1 w_2 \gamma_2 \delta_2 >_{6x1}$

Postmultiplying equation (23) by $A^{-1}$ yields:

$$\bar{F} = A^{-1}.B.\bar{\Delta} \quad (24)$$

or

$$\bar{F} = \bar{k}.\bar{\Delta} \quad (25)$$

Then

$$\bar{k} = A^{-1}.B \quad (26)$$

where $\bar{k}$ is the element stiffness matrix of dimension 6x6 relating end forces to end displacements in local coordinates.

Adding the axial stiffness, then

$$\{\bar{F}\}_{8x1} = [\bar{k}]_{8x8} \{\bar{\Delta}\}_{8x1} \quad (27)$$

where

$$\{\bar{F}\}_{8x1} = < N_1 Q_1 M_1 (M_1)_1 N_2 Q_2 M_2 (M_1)_2 > \quad (28)$$

$$\{\bar{\Delta}\}_{8x1} = < u_1 w_1 \gamma_1 \delta_1 u_2 w_2 \gamma_2 \delta_2 > \quad (29)$$

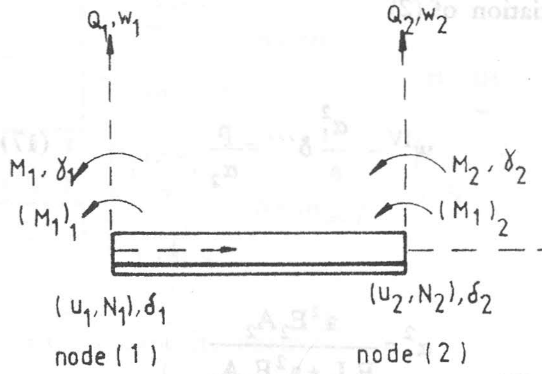


Figure 4. Plane composite beam element.

in which $N_1$, $N_2$ are the axial forces and $u_1$, $u_2$ are the axial displacements of the element at node 1,2, respectively.

The element stiffness matrix $[\bar{K}]_{8x8}$ is given in Appendix B.

## VERIFICATION OF THE MODEL

Two computer programs have been developed to implement both Transport Matrix Method and Finite Element Method described in the previous section.

To demonstrate the accuracy and efficiency of the proposed theoretical model, a comparison is made with some experimental results concerning different types of composite elements. For sandwich beams a comparison is made with the tests performed by Gehard Schuler [7]. On the other hand, reinforced concrete beams strengthened by epoxy-bonded steel plates is compared with the test performed by R.N. Swamy, R. Jones and J.W. Bloxham [8]. A good agreement between theoretical and experimental results is observed.

### *Example 1*

In the experiments performed by Gehard Schuler ten sandwich beam systems were tested. All beams have the same cross section given in Figure (5). The cross sections consists of two relatively thin steel faces and a foamed plastic core, the top face has a flexural rigidity and the bottom face is lightly profiled. The elastic modulus of steel used in faces is $2.1 \times 10^5$ N/mm$^2$. Other geometric values were as follows:

Thickness of upper steel face = 0.58mm, $\alpha_1^2 = 0.848$
Thickness of lower steel face= 0.5mm, $\alpha_2 = 1160414$ KN. cm$^2$.
Core thickness (a) = 52 mm, $E_2A_2 = 36387$ KN.

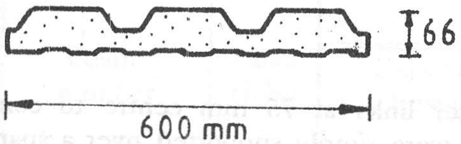


Figure 5. Cross section of sandwich beams.

The span of the beam system L ranged from 1000 mm to 1500 mm. To ensure the system continuity the beams were extended over the supports with a variable length $\eta L$, where $\eta$ varied from 0.049 to 0.333. For each of the beam systems several elements were tested. The researcher determined the factor $\omega$ for each beam system, which depends on the flexibility of the core together with the rigidity of other system parts, using the experimental esults and his own theoretical equations. The first five sandwich beam system were loaded by a concentrated load at the midspan while the other five beam systems were loaded at the third points of the span with two concentrated loads. The loading was in the elastic range with total loads not exceeding 3KN. The midspan deflection w was considered the average value of the results obtained from the several tested elements for each loading system. Table (1) and (2) show the experimental results for $\omega$ as well as the comparison between the theoretical values of the central deflection determined using the present theoretical model and those related to Schular experimental work. The percentage difference between the two results have a maximum value of 1.68% for the first group of beam systems and 0.49% for the second group. A very good agreement is observed.

Table 1. Comparison of the central deflection w for first group of beam systems.

| Beam Number | L(mm) | $\eta$ | Experimental value of $\omega$(1/cm) | Central deflection of the beam (mm) | | |
|---|---|---|---|---|---|---|
| | | | | Experimental results | Present theoretical model | Percentage relative difference |
| 1 | 1500 | 0.055 | 0.0126 | 4.812 | 4.893 | 1.68% |
| 2 | 1250 | 0.166 | 0.0134 | 3.143 | 3.139 | 0.13% |
| 3 | 1000 | 0.333 | 0.0138 | 1.879 | 1.882 | 0.16% |
| 4 | 1250 | 0.055 | 0.0123 | 3.362 | 3.371 | 0.27% |
| 5 | 1000 | 0.049 | 0.0118 | 2.138 | 2.114 | 1.12% |

Table 2. Comparison of the central deflection w for the second group of beam systems.

| Beam Number | L(mm) | $\eta$ | Experimental value of $\omega$(1/cm) | Central deflection of the beam (mm) | | |
|---|---|---|---|---|---|---|
| | | | | Experimental results | Present theoretical model | Percentage relative difference |
| 1 | 1500 | 0.055 | 0.0130 | 3.977 | 3.982 | 0.13% |
| 2 | 1250 | 0.166 | 0.0135 | 2.608 | 2.616 | 0.31% |
| 3 | 1000 | 0.333 | 0.0148 | 1.500 | 1.496 | 0.27% |
| 4 | 1250 | 0.055 | 0.0131 | 2.672 | 2.685 | 0.49% |
| 5 | 1000 | 0.049 | 0.0127 | 1.687 | 1.690 | 0.18% |

*Example 2*

In the tests performed by R.N. Swamy, R. Jones and J.W.Bloxham [8] nine beams were analyzed. All the beams were 155 x 255 mm in cross section and 2500 mm long. The beams were reinforced with 3 no. 20 mm diameter bars at an effective depth of 220 mm. The shear spans were provided with 6mm diameter links at 75 mm centre to centre. The beams were simply supported over a span of 2300 mm and loaded at the third points. the details of the beams are shown in Figure (6) and the details of the main variables in the tests are given in Table (3).

Table 3. Details of the Main Variables of the Test [8].

| Beam Number | 0 | 1 | 2 | 3 | 4 | 5 | 6 | 7 | 8 | 9 |
|---|---|---|---|---|---|---|---|---|---|---|
| Glue thickness(mm) | - | 1.5 | 1.5 | 1.5 | 3.0 | 3.0 | 3.0 | 6.0 | 6.0 | 6.0 |
| Plate thickness (mm) | - | 1.5 | 3.0 | 6.0 | 1.5 | 3.0 | 6.0 | 1.5 | 3.0 | 6.0 |
| Load at third points (KN) | 100 | 104 | 110 | 131 | 111 | 126 | 130 | 111 | 123 | 134 |

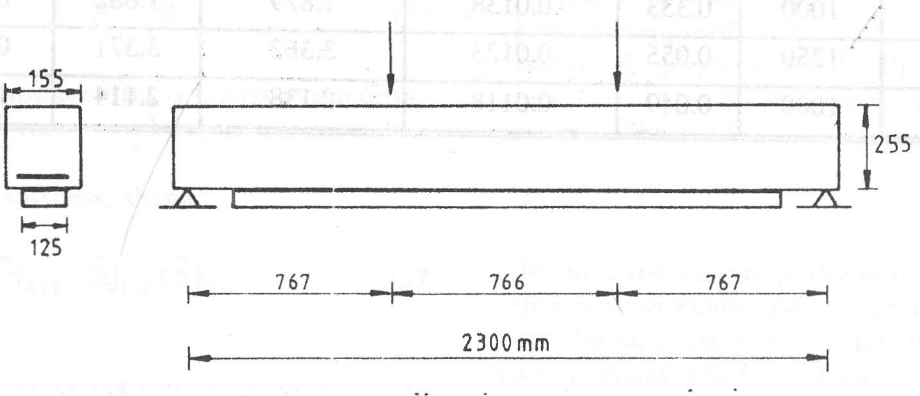


Figure 6. Details of test beams [8].

Table (4) shows comparisons between theoretical and experimental values of the central deflection of the beam. Swamy used the deflection of unplated beam (Beam No.o) loaded by two concentrated loads each of 100 KN as a reference (4.6mm). Then, for all other tests he forced the central deflection to take the same value of 4.6mm and estimated the corresponding loads.

In the present theoretical model, the flexural rigidity of the reinforced concrete element is taken corresponding to the experimental work for the unplated beam. This value is kept constant for all other beams. The considered elastic modulus of the epoxy resin is an average value at medium strain.

Table 4. Comparisons between theoretical and experimental results of R.C. Beam.

| Beam number | Load (KN) | Central Deflection of the Beam (mm) | | Percentage Relative Difference |
|---|---|---|---|---|
| | | Experimental Results [8] | Present Theoretical Model | |
| 0 | 100 | 4.600 | 4.600 | 0.00% |
| 1 | 104 | 4.600 | 4.528 | 1.57% |
| 2 | 110 | 4.600 | 4.541 | 1.28% |
| 3 | 131 | 4.600 | 4.885 | 6.20% |
| 4 | 111 | 4.600 | 4.827 | 4.93% |
| 5 | 126 | 4.600 | 5.190 | 12.83% |
| 6 | 130 | 4.600 | 4.829 | 4.98% |
| 7 | 111 | 4.600 | 4.814 | 4.65% |
| 8 | 123 | 4.600 | 5.042 | 9.61% |
| 9 | 134 | 4.600 | 4.940 | 7.39% |

In a plated reinforced concrete beam, the overall flexural rigidity of the composite structural member has no constant value, but varies with the applied load, degree of cracking, plate thickness, and glue thickness. Furthermore because of the viscoelastic nature of the adhesive, its modulus of rigidity varied with the intensity of the applied load. That explains the slight differences (1.28 to 12.83%) between the theoretical and experimental values where the beams had different loading degrees.

### *Design curves for sandwich beams*

Design curves for sandwich beams with top profiled face due to different cases of loading are obtained. These design curves are for simply supported beams, Figure (7) to Figure (10), as well as for fixed beams, Figure (11) to Figure (15). They may be helpfull for the optimum design for composite beams. Also, they can be used for obtaining the deformations and the internal forces in a short time rather than going through the complicated theoretical analysis.

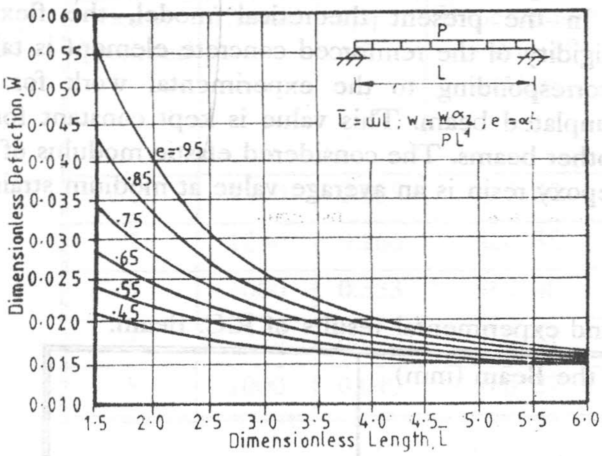


Figure 7. Design curves for sandwich beams with top profiled face.

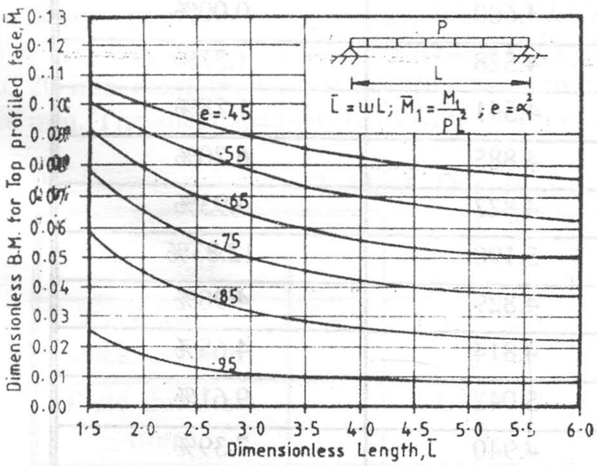


Figure 8. Design curves for sandwich beams with top profiled face.

All design curves are presented in dimensionless form. For each simply supported beam, the relations between the dimenionless length and the corresponding dimenionless central deflection and the positive bending moment of the top profiled face at the mid span of the beam are given. The cross section of the beam can take any dimensions. Six curves are presented in every chart for different values of $\alpha_1^2$. For every beam with fixed end three charts are given. Two of them are the same as in the simply supported beams while the third chart shows the relation between the dimenionless length and the corresponding dimensionless maximum negative bending moment at the end of the top profiled face.

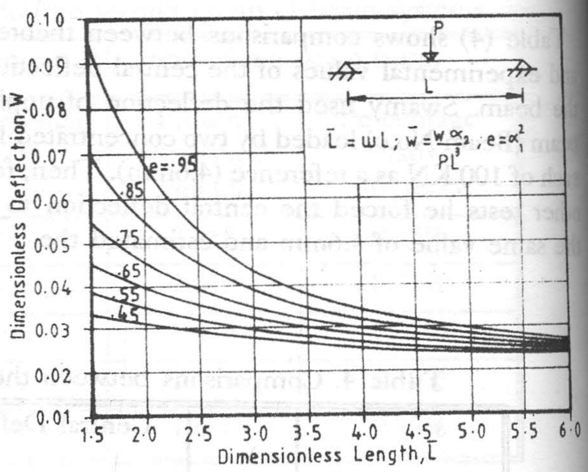


Figure 9. Design curves for sandwich beams with top profiled face.

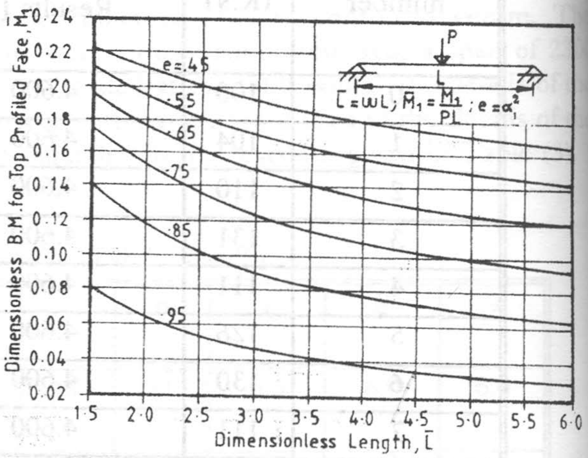


Figure 10. Design curves for sandwich beams with top profiled face.

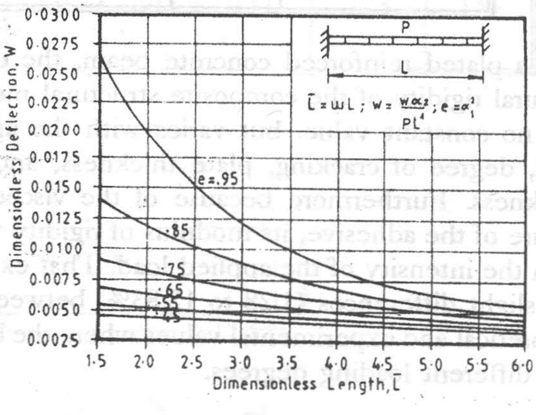


Figure 11. Design curves for sandwich beams with top profiled face.

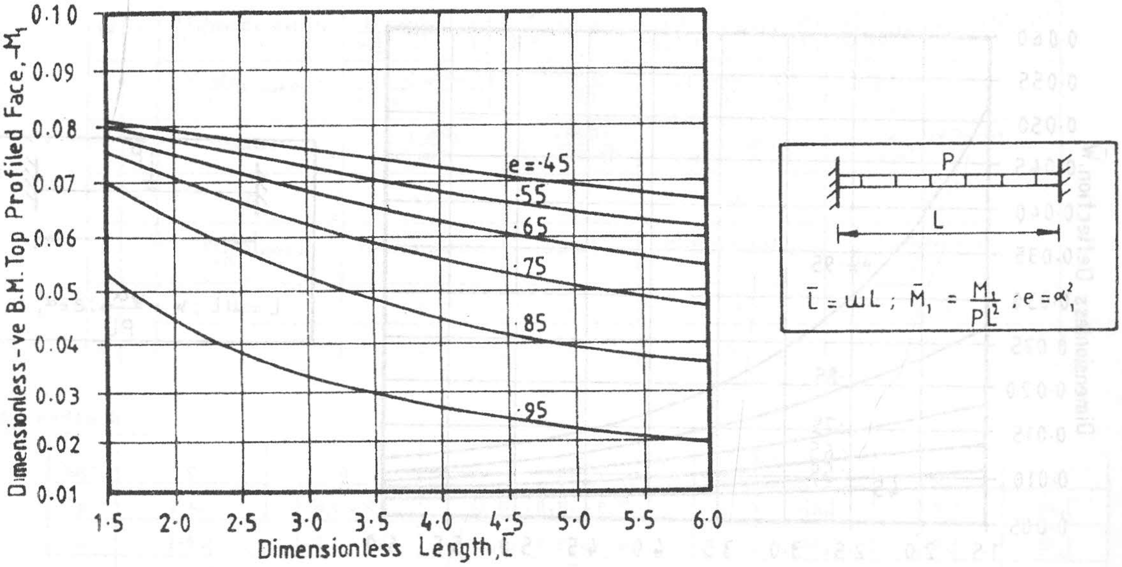


Figure 12. Design curves for sandwich beams with top profiled face.

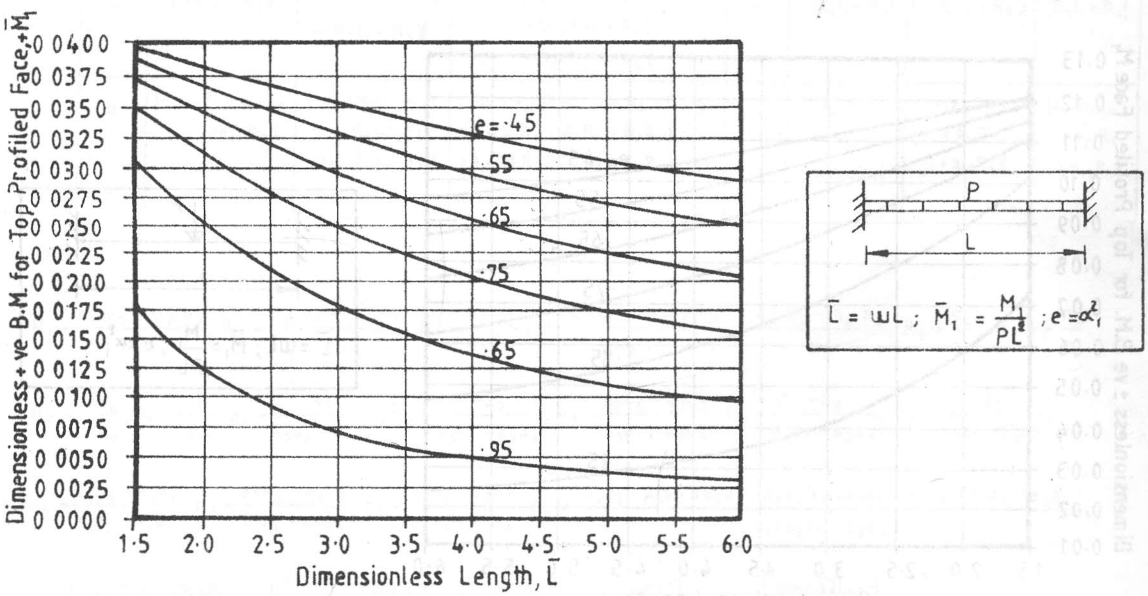


Figure 13. Design curves for sandwich beams with top profiled face.

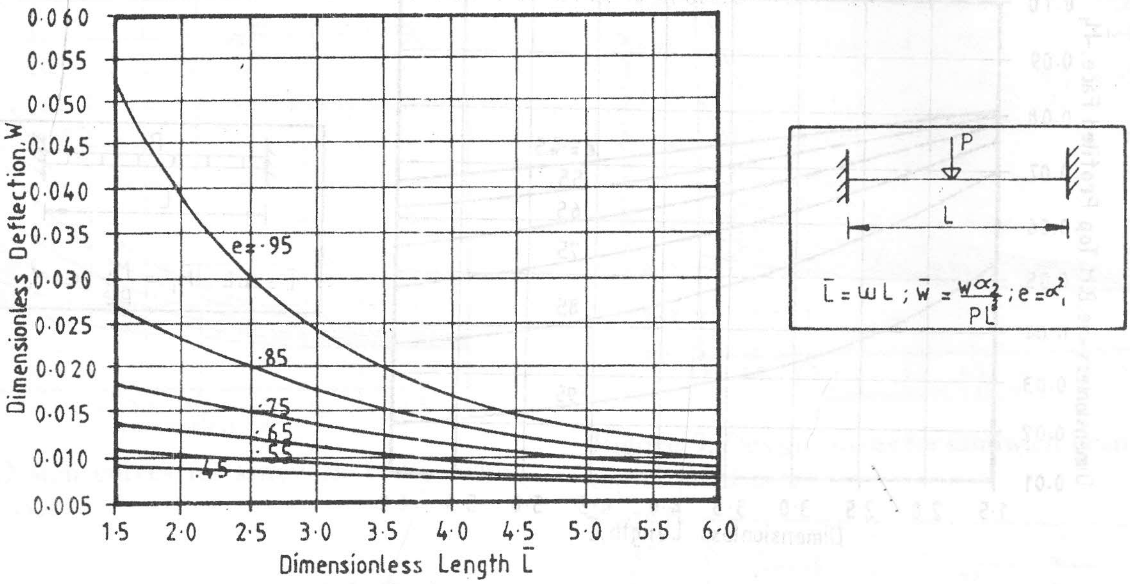


Figure 14. Design curves for sandwich beams with top profiled face.

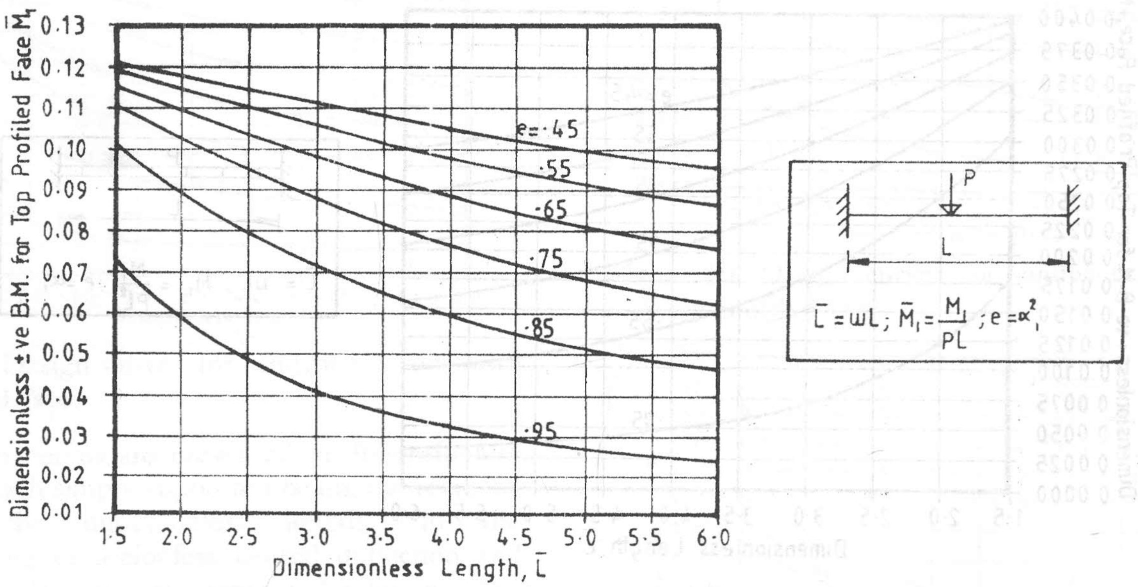


Figure 15. Design curves for sandwich beams with top profiled face.

## Appendix A

$$[T]_{7\times7}=\left[\begin{array}{c|c|c|c|c|c|c}
1.0 & x & \frac{1}{a\Omega}\left[\alpha_1^2(\sinh\Omega x-\Omega x)+\Omega x\right] & \frac{1}{\alpha_2}\left[\frac{\cosh\Omega x-1}{\Omega^2}-\frac{x^2}{2}\right] & \frac{1}{\alpha_2\omega^2}(1-\cosh\Omega x) & \frac{1}{\alpha_2}\left[\frac{\alpha_1^2}{\omega^2\Omega}(\Omega x-\sinh\Omega x)-\frac{x^3}{6}\right] & \frac{p}{\alpha_2}\left[\frac{\alpha_1^2}{\Omega^2\omega^2}\left(\cosh\Omega x-1-\frac{\Omega^2x^2}{2}\right)+\frac{x^4}{24}\right] \\ \hline
0 & 1.0 & \frac{(1-\alpha_1^2)}{a}(1-\cosh\Omega x) & \frac{-1}{\alpha_2}\left[\frac{1-\alpha_1^2}{\alpha_1^2}\frac{\sinh\Omega x}{\Omega}+x\right] & \frac{1}{\alpha_2}\cdot\frac{\sinh\Omega x}{\alpha_1^2\Omega} & \frac{1}{\alpha_2}\left[\frac{\cosh\Omega x-1}{\Omega^2}-\frac{x^2}{2}\right] & \frac{p}{\alpha_2}\left[\frac{\Omega x-\sinh\Omega x}{\Omega^3}+\frac{x^3}{6}\right] \\ \hline
0 & 0 & \cosh\Omega x & \frac{1}{\alpha_2}\cdot\frac{a\sinh\Omega x}{\alpha_1^2\Omega} & \frac{-1}{\alpha_2}\frac{a\sinh\Omega x}{\alpha_1^2\Omega(1-\alpha_1^2)} & \frac{a}{\alpha_2\omega^2}(1-\cosh\Omega x) & \frac{p.a}{\alpha_2\omega^2}\cdot\frac{\sinh\Omega x-\Omega x}{\Omega} \\ \hline
0 & 0 & 0 & 1.0 & 0 & x & \frac{-px^2}{2} \\ \hline
0 & 0 & \frac{-\alpha_2\alpha_1^2\omega^2}{a\Omega}\sinh\Omega x & (1-\alpha_1^2)(1-\cosh\Omega x) & \cosh\Omega x & \frac{\alpha_1^2(\sinh\Omega x-\Omega x)}{\Omega}+x & -p\left[\frac{\alpha_1^2(\cosh\Omega x-1)}{\Omega^2}+\frac{x^2}{2}(1-\alpha_1^2)\right] \\ \hline
0 & 0 & 0 & 0 & 0 & 1.0 & -px \\ \hline
0 & 0 & 0 & 0 & 0 & 0 & 1.0
\end{array}\right]$$

## Appendix B

$$\left[\bar{k}\right]_{8\times8}=\left[\begin{array}{c|c|c|c|c|c|c|c}
EA/L & 0 & 0 & 0 & -EA/L & 0 & 0 & 0 \\ \hline
0 & \left|-R_1\right| & \left|-R_1L+R_2\right| & \left|R_1B_1+R_2B_2+R_3B_3\right| & 0 & -\left|R_1\right| & \left|-R_2\right| & \left|R_3\right| \\ \hline
0 & \left|-R_4\right| & \left|-R_4L+R_5\right| & \left|R_4B_1+R_5B_2+R_6B_3\right| & 0 & -\left|R_4\right| & \left|-R_5\right| & \left|R_6\right| \\ \hline
0 & \left|-R_7\right| & \left|-R_7L+R_8\right| & \left|R_7B_1+R_8B_2+R_9B_3\right| & 0 & -\left|R_7\right| & \left|-R_8\right| & \left|R_9\right| \\ \hline
-EA/L & 0 & 0 & 0 & EA/L & 0 & 0 & 0 \\ \hline
0 & -\left|-R_1\right| & -\left|-R_1L+R_2\right| & -\left|R_1B_1+R_2B_2+R_3B_3\right| & 0 & \left|R_1\right| & -\left|-R_2\right| & -\left|R_3\right| \\ \hline
0 & \left|-(R_1L+R_4)\right| & \begin{array}{c}\left|-(R_1L+R_4)L\right.\\ \left.+(R_2L+R_5)\right|\end{array} & \begin{array}{c}\left|B_1(R_1L+R_4)\right.\\ +B_2(R_2L+R_5)\\ \left.+B_3(R_3L+R_6)\right|\end{array} & 0 & -\left|R_1L+R_4\right| & \left|-(R_2L+R_5)\right| & \left|R_3L+R_6\right| \\ \hline
0 & \begin{array}{c}\left|-(a_{10}R_1+a_{11}R_4\right.\\ \left.+a_{12}R_7)\right|\end{array} & \begin{array}{c}\left|-a_{10}(R_1L-R_2)\right.\\ -a_{11}(R_4L-R_5)\\ \left.-a_{12}(R_7L-R_8)\right|\end{array} & \begin{array}{c}\left|-B_4+a_{10}(B_1R_1+B_2R_2+B_3R_3)\right.\\ +a_{11}(B_1R_4+B_2R_5+B_3R_6)\\ \left.+a_{12}(B_1R_;+B_2R_8+B_3R_9)\right|\end{array} & 0 & \begin{array}{c}-\left|a_{10}R_1\right.\\ +a_{11}R_4\\ \left.+a_{12}R_7\right|\end{array} & \begin{array}{c}\left|-(a_{10}R_2\right.\\ +a_{11}R_5\\ \left.+a_{12}R_8)\right|\end{array} & \begin{array}{c}\left|a_{10}R_3\right.\\ +a_{11}R_6\\ \left.+a_{12}R_9\right|\end{array}
\end{array}\right]$$

where

$$R_1=\frac{n_1.n_9-n_7.n_3}{n_9},\ R_2=\frac{n_2.n_9-n_8.n_3}{n_9},\ R_3=\frac{n_3}{n_9},\ R_4=\frac{n_4.n_9-n_7.n_6}{n_9},\ R_5=\frac{n_5.n_9-n_8.n_6}{n_9},\ R_6=\frac{n_6}{n_9},\ R_7=-\frac{n_7}{n_9},$$

$$R_8=-\frac{n_8}{n_9},\ R_9=\frac{1}{n_9},\ n_1=\frac{a_5}{a_5a_1-a_2a_4},\ n_2=\frac{-a_2}{a_5a_1-a_2a_4},\ n_3=\frac{a_2a_6-a_3a_5}{a_5a_1-a_2a_4},\ n_4=\frac{-a_4}{a_5a_1-a_2a_4},\ n_5=\frac{a_1}{a_5a_1-a_2a_4},$$

$$n_6=\frac{a_3a_4-a_6a_1}{a_5a_1-a_2a_4},\ n_7=\frac{a_7a_5-a_4a_8}{a_5a_1-a_2a_4},\ n_8=\frac{a_8a_1-a_2a_7}{a_5a_1-a_2a_4},\ n_9=\frac{(a_9a_1-a_3a_7)(a_5a_1-a_2a_4)-(a_6a_1-a_3a_4)(a_8a_1-a_2a_7)}{a_1(a_5a_1-a_2a_4)},$$

$$a_1=\frac{\alpha_1^2(\Omega L-\sinh\Omega L)}{\omega^2\Omega\alpha_2}-\frac{L^3}{6\alpha_2},\ a_2=\frac{\text{cosn}\,\Omega L-1}{\alpha_2\Omega^2}-\frac{L^2}{2\alpha_2},\ a_3=\frac{1-\cosh\Omega L}{\alpha_2\omega^2},\ a_4=-\left[\frac{\cosh\Omega L-1}{\alpha_2\Omega^2}-\frac{L^2}{2\alpha_2}\right],$$

$$a_5=\frac{(1-\alpha_1^2)\sinh\Omega L}{\alpha_2\alpha_1^2\Omega}+\frac{L}{\alpha_2},\ a_6=-\frac{\sinh\Omega L}{\alpha_1^2\alpha_2\Omega},\ a_7=\frac{a(1-\cosh\Omega L)}{\alpha_2\omega^2},\ a_8=\frac{a\sinh\Omega L}{\alpha_2\alpha_1^2\Omega},\ a_9=-\frac{a\sinh\Omega L}{\alpha_2\alpha_1^2\Omega(1-\alpha_1^2)},$$

$$a_{10}=\frac{\alpha_1^2(\sinh\Omega L-\Omega L)}{\Omega}+L,\ a_{11}=(1-\alpha_1^2)(1-\cosh\Omega L),\ a_{12}=\cosh\Omega L,\ B_1=-\left[\frac{\alpha_1^2(\sinh\Omega L-\Omega L)}{a\Omega}+\frac{L}{a}\right],$$

$$B_2=\frac{1-\alpha_1^2}{a}(1-\cosh\Omega L),\ B_3=-\cosh\Omega L,\ B_4=\frac{\alpha_2\alpha_1^2\omega^2\sinh\Omega L}{a\Omega}.$$

## CONCLUSIONS

A theoretical model for the analysis of composite beam sections is presented. The considered composite section consists of two materials bonded together by a flexible bond layer. The top material has a flexural rigidity and the bottom material has an axial resistance only. The equations of equilibrium are developed and two methods of solution are utilized. These methods are: a-the Transport Matrix Method, TMM, and b- the Finite Element Method, FEM. Computer programs capable of analyzing both beams and frames are developed and checked.

Two types of composite sections are studied, sandwich beams with top profiled face and reinforced concrete beams strengthened by epoxy bonded steel plates. Comparisons with the results of the available experimental tests are provided. A good agreement between the theoretical and the experimental results is observed.

The analytical results are used to develop design curves for sandwich beams with top profiled face. Simply supported beams and fixed end beams are obtained for different loading cases.
Some general conclusions are deduced:

1- Composite beam and frame sections consist of two material bonded together by a flexible bond layer can be analyzed successfully by using the two proposed methods of solution TMM and FEM.
2- Both methods give identical values of deformations and internal forces.
3- The results of the theoretical model are within 0.13 to 12.83 percent of experimental results available in the literature.
4- For the proposed model, the relative shear deformation of the bond material has no effect on the total bending moment of the composite beam.
5- The obtained design curves enables the design engineer to control the expected sandwich beam deflection by decreasing the cross-section profile, $\alpha_1^2$ or increasing the rigidity of the core, $\omega L$. However, the internal forces can be controlled by increasing the cross-section profile, $\alpha_1^2$, or increasing the rigidity of the core, $\omega L$.

## REFERENCES


[1] Y. Frosting, "Behavior of Delaminated Sandwich Beam with Transversely Flexible Core-High Order Theory", *Composite Structures,* vol. 20, pp. 1-16, 1992.

[2] O. Vilnay, "The Behavior of Aluminum Alloy Struts and Beams Reinforced by Adhesive Bonding of Carbon Fibre/Epoxy Composite", *International Conference on Steel and Aluminum Structures*, pp. 135-144, 1987.

[3] T.V. Parry and Wronski, "Selective Reinforcement of an Aluminum Alloy by Adhesive Bonding with Uniaxially Aligned Carbon Fiber/Epoxy Composites", *Composites,* October, pp. 249-255, 1981.

[4] F.J.H. Tutt, Bsc, Mimeche, "Carbon Fibre Reinforcement of Experimental Military Bridge Structures", *Institution of Civil Engineers*, pp. 211-219, 1977.

[5] R. Jones, R.N. Swamy and A. Charif, "Plate Separation and Anchorage of Reinforced Concrete Beams Strengthened by Epoxy-Bonded Steel Plates", *The Structural Engineer*, 66, No. 5, March, pp. 85-94, 1988.

[6] T.M. Roberts, "Approximate Analysis of Shear and Normal Stress Concentrations in the Adhesive Layer of Plated RC Beams", *Journal of the Institution of Structural Engineers,* vol. 67, June, pp. 229-233, 1989.

[7] Gehard Schuler, "Durchlaufträger mit Elastischem Verbund bei Abschnittsweise veränderlichen Steifigkeiten", Dissertation, Karlsruhe Universität, 1986.

[8] R.N. Swamy, R. Jones, J.W. Bloxham, "Structural Behavior of Reinforced Concrete Beams Strengthened by Epoxy-Bonded Steel Plates", *The Structural Engineer*, 65A, No. 2, February, pp. 59-68, 1987.